Magnetic Resonance Force Microscopy and the spin bath : towards single-spin massive-resonator entanglement and the spoiling influence of the spin bath

Voogd, J.M. de

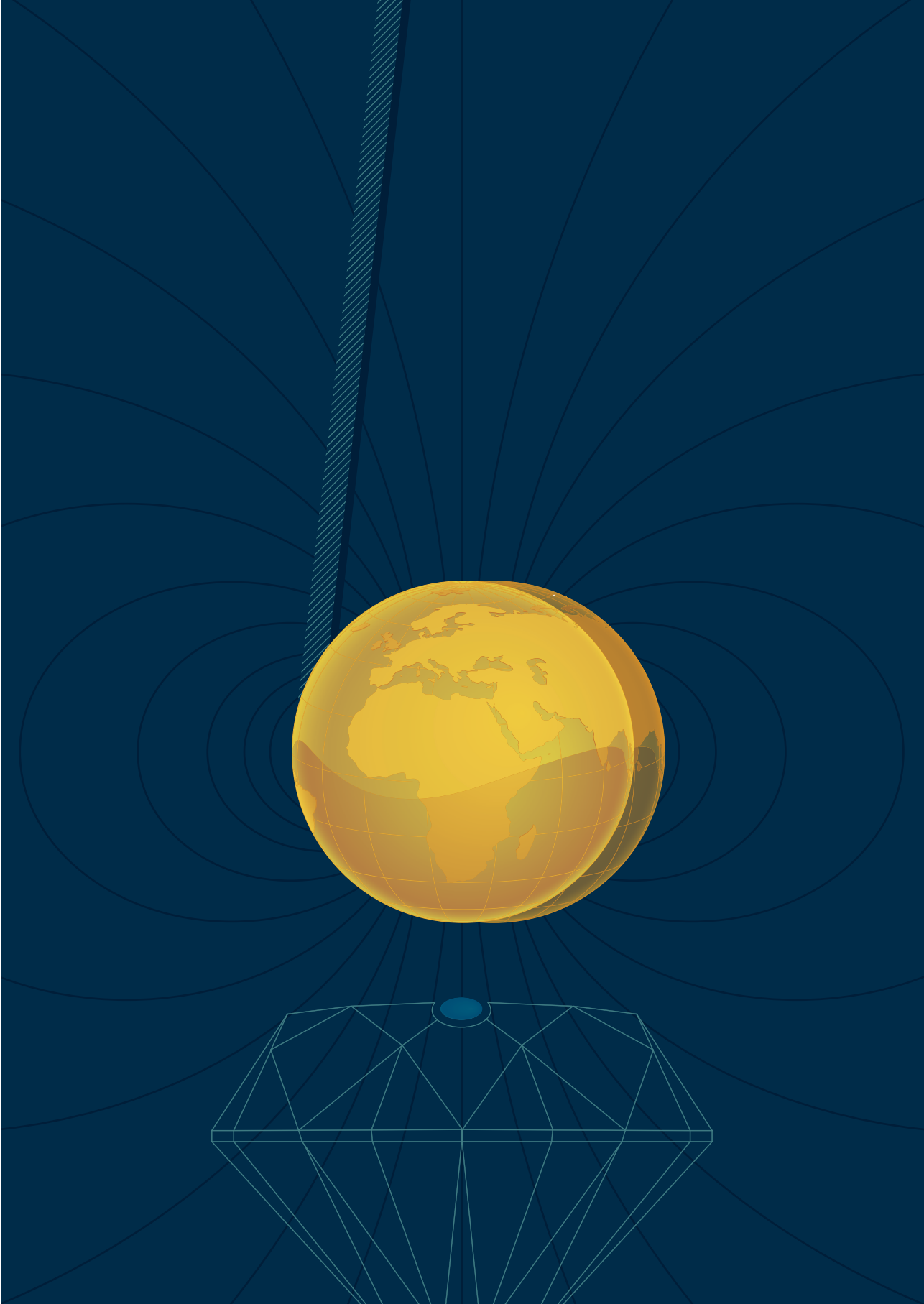

5 *Gravitational decoherence of NV-resonator systems*

quote Rabi 1970

"Science itself is badly in need of integration and unification. The tendency is more and more the other way... Only the graduate student, poor beast of burden that he is, can be expected to know a little of each. As the number of physicists increases, each specialty becomes more self-sustaining and self-contained. Such Balkanization carries physics, and, indeed, every science further away from natural philosophy, which, intellectually, is the meaning and goal of science."

As described in Ch. 1, the goal of the proposal that led to this thesis is clear; an experiment that verifies or falsifies gravitational collapse models would have major implications for the physicist's perceived worldview. Besides that an experiment like this would enlighten the almost century-old discussion about the correct interpretation of quantum mechanics, it could also point towards the right way to unify the theories of gravity and quantum mechanics. As Rabi states in the quote above, science needs unification but tends to disperse into different fields, branches, and subbranches.
To design such an experiment we need to work the other way around and collect the expertise of many branches to overcome technical and theoretical challenges. As Rabi also mentioned, a PhD-student can be expected to extract the information of all the necessary fields, albeit that he or she might have too little time to design a well defined exper-

iment. Therefore this chapter is different from the others: instead of trying to draw firm conclusions we end most sections with an emphasized question, which is meant to guide successive research.

In the first three sections we will discuss the effect of the possible gravitational collapse effect onto the MRFM-resonator. The first section will review the original gravitational collapse theory as founded by Diósi and Penrose.[1,2] Next, we will suggest a modification predicting that the boundaries between quantum and classical mechanics occur for much smaller masses. The third section will review the proposed[3,4] effect of heating due to spontaneous collapse of the wave function.

[1] Diósi 1989
[2] Penrose 1996

[3] Bassi et al. 2013
[4] Vinante et al. 2016

The last two sections focuses on the experiment as suggested by Van Wezel and Oosterkamp 2012,[5] in which a well controlled spin should entangle with a massive resonator, hence creating a massive superposition. Sec. 5.4 will point out the relevant quantum mechanical interactions in this experiment that need to be understood very well to be able to measure a deviation from conventional quantum mechanics. Moreover, the quantum interactions are needed to push the system out of the safe regime of quantum mechanics. Finally, in Sec. 5.5 we describe the possibilities to concretely construct the experiment.

[5] Wezel and Oosterkamp 2012

As this is the last scientific chapter regarding the main subject of this thesis, we will make up the balance in Sec. 5.6 and also look ahead in this last section.

5.1 *Gravitational collapse*

In the Copenhagen interpretation of quantum mechanics, if one measures an observable of a quantum state, the classical measurement apparatus lets the wave function collapse. This means that the quantum state is reduced to an

eigenvalue of the observable.[6] It is, however, not clear what a classical apparatus precisely does or what classical even means. If the large amount of degrees of freedom in this apparatus are entangled with the measured state, does that mean that for each possibility there is another reality? Or does the state collapse, i.e. it chooses one reality? In the next section we will discuss that the first interpretation is not falsifiable, while collapse mechanisms lead to non-unitary quantum mechanics.

[6] In the case of a perfect position measurement, which we will be interested in, the wave function collapses to a delta function.

THE QUALITATIVE SOLUTION suggested by Diósi,[1] Penrose,[7] and many others,[3,8,9] is that the concept of gravity induces non-unitary behavior, which then leads to spontaneous collapse. Note that we work at non-relativistic speeds and in an almost flat spacetime. In other words, our physics consists of non-relativistic quantum mechanics and a weak gravitational field, albeit we will investigate what might happen when the gravitational field is generated by a mass in superposition. This conservative field can be described by the gradient of the gravitational potential $\Phi(\boldsymbol{r})$. For weak fields, the potential can be written as a first order perturbation to the flat spacetime.[10] Hence the local elapsed time interval $d\tau$ (proper time) becomes

$$d\tau = \left(1 + \frac{\Phi(\boldsymbol{r})}{c^2} + ...\right) dt, \tag{5.1}$$

where c is the speed of light and dt the time interval of an infinitely far away observer (coordinate time).[11] As Φ is always negative at finite distance of a massive object, the proper time is always slower than the coordinate time.

The gravitational potential is related to the mass distribution by Poisson's equation, which in integral form can be written as

$$\Phi(\boldsymbol{r}) = -G \int_{\mathbb{R}^3} d^3r' \, \frac{\rho(\boldsymbol{r}')}{|\boldsymbol{r} - \boldsymbol{r}'|}, \tag{5.2}$$

where G is the gravitational constant.

[7] Penrose 2014

[8] Oosterkamp and Zaanen 2013

[9] Rademaker et al. 2014

[10] Carroll 2003, Sec. 4.1

[11] The far away observer and the local experiment do not move (significantly) with respect to each other, so special relativistic effects can be neglected.

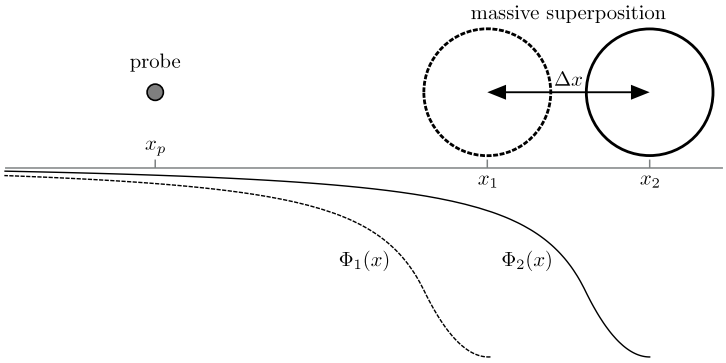

Figure 5.1: A massive ball is brought into a superposition of states at positions x_1 and x_2. This leads to a superposition of the gravitational potentials $\Phi_1(x)$ and $\Phi_2(x)$. Is the probe particle at position x_p in a superposition of spacetimes or does it experience a superposition of time evolutions? *Figure reprinted from Rademaker et al. 2014.*

The mass density ρ is trapped inside the gravitational potential as it costs works to remove each bit of mass. The total work to move each infinitesimal part from its current position to infinity is, up to a minus sign, the so called binding energy, E_b, which is given by

$$\begin{aligned} E_b &= \frac{1}{2}\int_{\mathbb{R}^3} d^3r\ \Phi(\boldsymbol{r})\rho(\boldsymbol{r}) \\ &= -\frac{G}{2}\int_{\mathbb{R}^3} d^3r \int_{\mathbb{R}^3} d^3r'\ \frac{\rho(\boldsymbol{r})\rho(\boldsymbol{r}')}{|\boldsymbol{r}-\boldsymbol{r}'|}. \end{aligned} \tag{5.3}$$

To SEE what parameters need to be optimized for measuring a gravitationally induced collapse of the quantum state, we need to ask ourselves how gravity sees the mass of the wave function. In quantum mechanics a particle is assigned a mass, but it does not tell how this mass is distributed over space. In other words, for choosing the right experiment we should know how the gravitational potential $\Phi(\boldsymbol{r})$ and a wave function $\Psi(\boldsymbol{r})$ are connected. However, here we encounter the 100 year old conundrum of the unfeasible unification of theory of gravity and quantum mechanics. As there is no answer known to how the gravitational potential is formed around a quantum state, let us revisit some possibilities. To stay close to our MRFM-experiment, we will evaluate the possibilities on a massive ball that is in a Schrödinger cat state as shown

in Fig. 5.1. Hence, we could write the quantum state as

$$|\Psi\rangle = \frac{1}{\sqrt{2}}\left(|1\rangle + |2\rangle\right), \tag{5.4}$$

where $|1\rangle$ and $|2\rangle$ correspond to the states with the center of mass of the ball at positions x_1 and x_2 respectively. If we assume that gravity does not know about 'mass distributions of quantum states', but rather is constructed for each possible outcome, we end up with two gravitational fields: Φ_1 and Φ_2 respectively.

It was argued by Penrose,[2] that an uncertainty in the gravitational binding energy occurs when the mass distribution is in a superposition. The lifetime that is associated with this state due to this uncertainty is guessed by dimensional analysis to be

$$\text{lifetime} = \frac{\hbar}{|E_\Delta|}. \tag{5.5}$$

The uncertainty energy E_Δ is some energy measure that can be related to the gravitational binding energy difference between the two possible outcomes of a two-state superposition

$$E_\Delta = -4\pi G \int_{\mathbb{R}^3} d^3r \int_{\mathbb{R}^3} d^3r' \, \frac{\left(\rho_1(\boldsymbol{r}) - \rho_2(\boldsymbol{r})\right)\left(\rho_1(\boldsymbol{r'}) - \rho_2(\boldsymbol{r'})\right)}{|\boldsymbol{r} - \boldsymbol{r'}|}, \tag{5.6}$$

where $\rho_1(\boldsymbol{r})$ and $\rho_2(\boldsymbol{r})$ are the mass densities that correspond with Φ_1 and Φ_2 respectively. A similar quantity was suggested by Diósi[1] a few years earlier. In Fig. 5.2 we plotted $\frac{\hbar}{E_\Delta}$ for our NdFeB magnetic particle of 1.5 μm radius as a function of superposition distance Δx. The Δx values shown here are way too large to be feasible, and the lifetimes far too long to be measured with current techniques. *If this is the macroscopic boundary of quantum mechanics, why is it so incredible hard to get the MRFM-tip into a quantum superposition even on millisecond timescales?* An often-heard answer argues that this is due to the coupling to environmental degrees of freedom which makes it difficult to prove superposition in an interference experiment. However, this does not explain the single

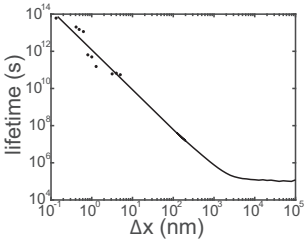

Figure 5.2: Numerical calculation of the Penrose collapse time for a magnet in a position cat state with a separation of Δx between the two states of which the total wave function is a superposition. The ball is of diameter 3 μm, similar to the size of the magnet as used in our MRFM experiment. For Δx values larger than $\sim$ 3 μm the two states do not overlap anymore. The line starts to flatten due to the trade-off of larger separation between the two states and weaker gravitational field that is generated by one state around the other. The shown points at small Δx that deviate from the straight line asymptote are due to numerical errors because of the large difference in scale between object size and Δx. Around these points the straight line is merely a guide to the eye.

outcome of measurements of quantum states.[12] In the next section we will argue that the rate might be much faster than in Eq. 5.6 as not only the mass from the object itself counts but also all other masses that feel the gravitational potentials from the massive quantum object.

[12] The environmental decoherence can explain the diagonalization of the density operator, however it does not explain why the remaining diagonal values are *probabilities*, i.e. why we have only one outcome per measurement.

5.2 *Probing the instability of a quantum superposition of time dilations*

This section is based on and continues on: Rademaker, L *et al.* Probing the Instability of a Quantum Superposition of Time Dilations. arXiv:1410.2303 [quant-ph] (2014).

So far we have looked at the massive object in superposition itself. However, it also changes the spacetime at the position of other objects. Compared to Diósi's and Penrose's ideas, including the surrounding mass is of vital importance. We demonstrate in this section on what typical timescales ordinary quantum mechanics might fail when not only the gravitational self energy of the object in superposition itself, but also the surrounding mass is taken into account. For calculating the time evolution of objects near a mass in superposition in the quantum domain, we should have a valid theory of quantum gravity. However, such a theory does not yet exist. Therefore, in order to find the typical timescale on which the quantum world becomes classical, we follow the reasoning from Oosterkamp and Zaanen 2013[16] where, based on a gedankenexperiment, they argue at which timescale the gravitational time dilation might force a collapse of the wavefunction, which turns out to be similar to the Diósi-Penrose interpretation. In contrast to that paper, we will include the effect of all surrounding mass.

Consider a probe particle at position x_p as shown in Fig. 5.1. Later on we will assume that the surrounding mass exists of many noninteracting probe particles. If the probe particle is subject to a time-independent Hamiltonian, its time-

dependent wave function can be written as

$$\left|\Psi_p(t)\right\rangle = e^{-i\hat{H}\tau/\hbar}\left|\Psi_p(0)\right\rangle. \tag{5.7}$$

Here $\hat{H}$ is the Hamiltonian (without gravity) and τ is the proper time from Eq. 5.1 which is equal to t in flat space. But spacetime is not flat and the neighboring massive object causes the probe particle's time to run slower. The problem is that a cat state of the massive object causes the proper time to be in superposition as well.

Let us consider the total quantum state of the probe particle $\left|\Psi_p\right\rangle$ and that of the massive object in superposition $|\Psi_M\rangle$ (with $|\Psi_M(0)\rangle = \frac{1}{\sqrt{2}}(|1\rangle + |2\rangle)$), where we assume that $\left|\Psi_p\right\rangle$, $|1\rangle$, and $|2\rangle$ are eigenstates of the position operator. When the particles do not interact[13] the total quantum state is

$$|\Psi(t)\rangle = \frac{1}{\sqrt{2}}e^{-i\hat{H}_M\tau_M/\hbar}\Bigg(|1\rangle\, e^{-i\hat{H}_p t\left(1+\frac{\Phi_1(x_p)}{c^2}\right)/\hbar} + |2\rangle\, e^{-i\hat{H}_p t\left(1+\frac{\Phi_2(x_p)}{c^2}\right)/\hbar}\Bigg)\left|\Psi_p(0)\right\rangle. \tag{5.8}$$

Note that the gravitational field acts on the probe particle's state as an operator with eigenvalues $\Phi_1(x_p)$ and $\Phi_2(x_p)$ for the position eigenstates. In fact, we also could have quantized the gravitational potential and included this into a new Hamiltonian $\hat{H}_{\text{with }\hat{\Phi}} = \hat{H}(1 + \frac{\hat{\Phi}}{c^2})$. For the result of Eq. 5.8 we neglected the fact that $\hat{H}$ and $\hat{\Phi}$ do not commute, as this only gives errors on the order of $\left(\frac{G}{c^2}\right)^2$.

So what we actually have done is quantizing gravity. However, this leads to a whole set of problems as explained in a review by Isham 1993.[14]

Of course, we could assume that for all positions of the massive quantum object in superposition we have a completely disjointed spacetime.[15] Assuming the superposition started at $t = 0$, the phase factor of the probe particle's wave function evolves in each spacetime differently. In this section we note that besides the probe particle, all surrounding matter continues in these spacetimes as well, including the measurement

[13] The total Hamiltonian (without gravity) of two non-interaction states can be written as a sum of two commuting parts $\hat{H} = \hat{H}_M + \hat{H}_p$. In flat space, the total quantum state would simply be $|\Psi\rangle = |\Psi_M\rangle\left|\Psi_p\right\rangle = e^{-i\hat{H}t/\hbar}\left|\Psi_M(0)\right\rangle\left|\Psi_p(0)\right\rangle$, where we omitted the direct-product sign for simplicity.

[14] Isham 1993

[15] A.k.a. a many worlds formalism.

apparatus and the observer. When a measurement is performed, the outcome depends on the spacetime the observer is in. Since all possible outcomes fully exist, it is not clear what the probability distribution $|\Psi(x)|^2$ physically means, other than some Bayesian probability for how much the observer continues to a certain 'world'. Also, this many worlds formalism is a non-falsifiable theory because ultimately we would consider a system consisting of a quantum system together with its measurement apparatus. The two possible outcomes of a measurement would then remain evermore in separate parts of the Hilbert space.

Note that the problems that arises due to the quantization are connected to the problematic straightforward unification of gravity and quantum theory, while the non-falsifiability of the many worlds interpretation touches the measurement problem in quantum mechanics. And so, although Eq. 5.8 is the most straightforward construction of the time evolution of the quantum state from a quantum mechanical and general relativity point of view, the problems above speak against it. However, we know that quantum mechanics works very well on small time scales. So instead of abandoning Eq. 5.8 we continue with this naive solution and try to estimate on what typical timescale things go awry. Oosterkamp and Zaanen 2013[16] followed the same approach, but they focused on the proper time of the massive object itself; the τ_M term in Eq. 5.8. They argued, based on the possible truly classical nature of the gravitational field (spacetime) that the phase difference between the two states of the massive object gives a measure of the collapse time. Doing so they found an expression very similar to Penrose's and Diósi's.

[16] Oosterkamp and Zaanen 2013

In our case, we do not consider the phases of the states of the massive object explicitly, but rather the states of the surrounding mass, starting with a single probe particle. Applying the same arguments[16,17] we find that quantum mechanics becomes ill-defined when the phase difference between

[17] Rademaker et al. 2014

the probe particle's state in either of the two spacetimes is $\pm\pi$, i.e.

$$\frac{Et}{\hbar c^2}\left(\Phi_1(\boldsymbol{x}_p) - \Phi_2(\boldsymbol{x}_p)\right) = \pm\pi, \tag{5.9}$$

where E is approximately[18] the energy of the state. To evaluate Eq. 5.9 for our experiment, we must know the energy.[19] Gravity is not so selective on the type of energy, so we use the by far dominant term to the particle's energy which is $E = m_p c^2$, with m_p the probe particle's mass.[20] It follows that the time it takes for the state of the collapse equals

$$\tau_p = \frac{\pi\hbar}{m_p\left|\Phi_1(\boldsymbol{x}_p) - \Phi_2(\boldsymbol{x}_p)\right|}. \tag{5.10}$$

Note that although we derived τ_p as a typical measure of the lifetime of the probe particle, it actually also limits the lifetime of the superposition of the heavy quantum object that generates the two spacetimes.[17] Thus in the case of multiple probe particles, we sum over the probe masses in the appropriate positions. If the superposition starts at $t = 0$, the spacetime can only be in superposition within a radius of $c\tau_p$ as the fabric of space can only change at the speed of light. This leads to a self-consistent equation which, when written as a continuous sum over the environment (probe particles), is given by

$$\tau_p = \frac{\pi\hbar}{\int_{|\boldsymbol{r}|\leq c\tau_p} \mathrm{d}^3 r \rho_p(\boldsymbol{r})\left|\Phi_1(\boldsymbol{r}) - \Phi_2(\boldsymbol{r})\right|}. \tag{5.11}$$

This typical measure of the gravitational induced decoherence time is calculated for our MRFM-tip where we took the earth as the environment. The obtained values for τ_p, shown in Fig. 5.3, are extraordinarily small compared to the values of Sec. 5.1. For example, for the same size of massive object, we now find a value of 4 μs for a superposition width of the size of the zero point motion. Note that any quantum state has a quantum uncertainty of at least this size. *This brings us to the question if there is not already an experiment done that shows signatures of the collapse time τ_p.* Certainly if the topic of the

[18] Remember that $|\Psi_p\rangle$ is not an eigenstate of the Hamiltonian. However, the difference in energy between various states is small compared to the dominant term and we can neglect these differences.

[19] This is the absolute energy, as explained in Oosterkamp and Zaanen 2013.

[20] It can be expected that for normal down-to-earth systems, the mass is the dominant term for the energy eigenstates used, thus making the assumption that $|\Psi_p(0)\rangle$ is an eigenstate of the Hamiltonian redundant.

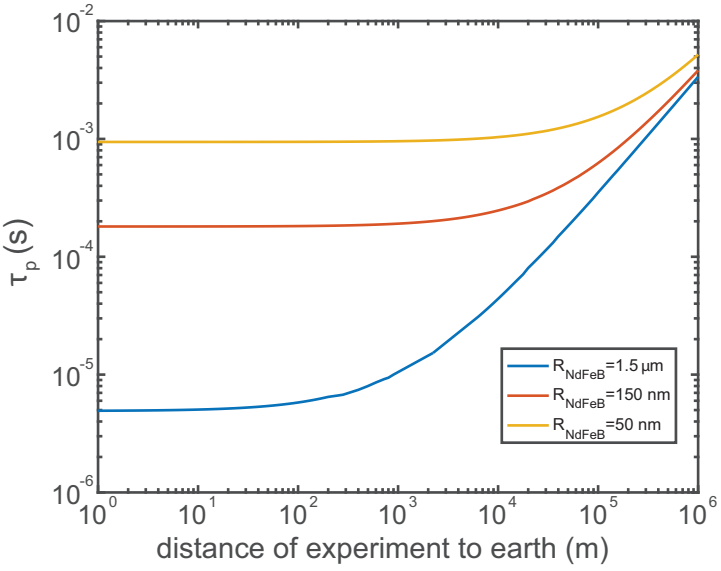

Figure 5.3: The typical measure of instability time τ_p for different distance to earth. The values are found by solving $\tau_p - \frac{\pi\hbar}{\int_{|r|\leq c\tau_p} \mathrm{d}^3 r \rho_p(r)|\Phi_1(r)-\Phi_2(r)|} = 0$ in MATLAB. The calculation is done for tip diameters of 3 µm, 300 nm, and 100 nm of NdFeB. The width of the superposition was set to the zero point motion of a typical MRFM-cantilever $x_{zpf} \approx 141$ fm.

next section is valid and taken into account, it is likely that signatures of the collapse time are already measured. Hence it could also be that Eq. 5.11 is falsified already. However, keep in mind that the generalization of Eq. 5.10 to Eq. 5.11 is based on the assumption that we can simply integrate over the probe particles mass distribution, which might not be valid.[21]

[21] For example, instead of summing over the probe particle's phases of Eq. 5.9, one might also take the root mean square of these phases. This would lead to a slower collapse time.

5.3 *Mode heating due to spontaneous wave function collapse*

Once the wave function collapses, naturally the kinetic energy of the system increases.[3,22,23] Roughly speaking, this is because the collapsed state will on average have a higher energy than the energy expectation value of the original state and it will release this energy as heat into the resonator when the system evolves in time.[24] The resonator can loose its heat-energy to the environment only if there is a temperature difference, similar to what is described in Sec. 1.4.

[22] Diósi 2015

[23] Diósi 2014

[24] In principle into the qubit-resonator system, but since the resonator has much higher heat capacity, the energy stored in the spin-part is insignificant. The heat-energy flow from the resonator to the environment through the spin is already included by means of the effective Q-factor.

Diósi 2015 calculated the temperature raise for the Diósi-Penrose model type of spontaneous wave function collapse $\Delta T \sim \frac{\hbar Q}{k_B \omega_0 \tau_p^2}$,[25] assuming that $k_B T \gg \hbar\omega_0$. For the largest magnet from Fig. 5.3, and our standard resonator values of $Q \sim 10^4$ and $\frac{\omega_0}{2\pi} = 3$ kHz, we find $\Delta T \sim 10^{-2}$ K which is larger than the offset measured by Vinante et al. 2016[4], but similar to the saturation temperature in both the Vinante and our experiments.[26]

The heating effect does not only apply to a resonator in the quantum regime, but provides a lower boundary for the temperature of any resonator, also in the classical regime. In Sec. 4.2 we found a saturation of the mode temperature around 50 mK that we ascribed to vibrations or other noise sources. Usenko et al. 2011 found a saturation at similar temperatures.[27]

That Vinante et al. 2012 reached lower temperatures by doing active feedback does not contradict the above numbers as the active feedback signal does not tell if the heat input comes from the temperature difference between the heat bath and the environment, from vibrations in the system, or from spontaneous collapse.

The relevant question for our experiment is whether this intrinsic heating might prevent the cooling of the system towards the ground state. If yes, then we are very close to observing the effects of spontaneous wave function collapse. If in the proposed experiment we find that there is no significant intrinsic heating, this would either disprove the assumption on which the heating is based, or ask for modifications or exclusion of some spontaneous collapse models (not only the modified Diósi-Penrose model from Sec. 5.2).[4]

[25] This comes from Eq. 16 in Diósi 2015: $\Delta T \sim \frac{\hbar\omega_G^2}{2k_B}\tau$, where $\tau = \frac{Q}{\omega_0}$ is the cantilever time constant and $\omega_G \sim \frac{1}{\tau_p}$, the inverse of the collapse time.

[26] Usenko et al. 2011

[27] Which they attribute to black body radiation from a 4K thermal shield that heat up the force sensor.

We can conclude that the masses and oscillation periods of the conventional MRFM-tips fall precisely in the regime where, following the model of Sec. 5.2, the transition occurs from the quantum to the macroscopic world. This chap-

ter will elaborate on the construction of an experiment to test this and other spontaneous collapse models. It must be noted, however, that the theory of Secs. 5.1-5.3 is based on various assumptions and generalizations that are not straightforward. There are many other routes possible in which gravitation might induce an uncertainty into the quantum state.[3] What we really need in this field is an experiment.

5.4 *Quantum description of spin - resonator system*

So far we have checked how the spin-resonator system could be pushed over the boundaries of quantum mechanics. However, we should also know how the experiment would be described in a purely quantum formalism. Firstly because we need quantum mechanics to push the system towards the quantum/classical boundaries, and secondly because we need to have a reference for our results once the experiment passes the boundaries.

The Hamiltonian of the coupled resonator - spin system is given by

$$H = \frac{1}{2m}p^2 + \frac{1}{2}kq^2 + \omega_s \boldsymbol{B}(q) \cdot \boldsymbol{S}, \tag{5.12}$$

where p and q are the resonators canonical momentum and position variable respectively, m the mass of the resonator, k the spring constant, ω_s the Larmor frequency, and $\boldsymbol{S}$ the orientation of the spin.

The magnetic field $\boldsymbol{B}$ can be expanded to first order in q. Higher orders can be omitted if the spin is positioned such that $\frac{\partial^2 \boldsymbol{B}}{\partial q^2} \ll \frac{2\boldsymbol{B}'}{q_{ZPF}}$, where $\boldsymbol{B}' \equiv \frac{\partial \boldsymbol{B}}{\partial q}$, $q_{ZPF} \equiv \sqrt{\frac{\hbar}{2m\omega_0}}$ the ground state energy motion (zero point fluctuation in position), and $\omega_0 = \sqrt{\frac{k}{m}}$ the cantilever's natural frequency. The magnetic field can be expanded as $\boldsymbol{B} \approx B_0\hat{\boldsymbol{z}} + q\boldsymbol{B}'$ where we have chosen a Cartesian basis with $\hat{\boldsymbol{z}} = \frac{\boldsymbol{B}(q=0)}{B_0}$.[28] Quantizing the

[28] Note that xyz is a local basis for the qubit and is not related to the commonly chosen basis in MRFM-experiments such as in Fig. 3.1 or 4.12.

Hamiltonian leads to

$$\hat{H} = \hbar\omega_0 \left(\hat{a}^\dagger \hat{a} + \frac{1}{2}\right) + \omega_s \hat{S}_z + \left(\hat{a}^\dagger + \hat{a}\right)\left(g_\perp^* \hat{S}_+ + g_\perp \hat{S}_- + g_\parallel \hat{S}_z\right), \tag{5.13}$$

where $\hat{a}^\dagger \equiv \frac{1}{2q_{ZPF}}\left(\hat{q} - \frac{i}{m\omega_0}\hat{p}\right)$ and $\hat{a}$ the creation and annihilation operators respectively. Furthermore, $g_\parallel \equiv -\gamma_s q_{ZPF} B'_z$, and $g_\perp \equiv -\gamma_s q_{ZPF}\left(B'_x + iB'_y\right)$. $\hat{S}_x, \hat{S}_y$ and $\hat{S}_z$ are the spin operators and $\hat{S}_\pm = \hat{S}_x \pm i\hat{S}_y$ the spin raising and lowering operators.

Up to now, the Hamiltonian is general enough for any spin number. For simplicity let us focus on a two level system (2LS).[29] Taking the ground state as zero energy, we can write $\hat{S}_z = \hbar\hat{\sigma}^\dagger\hat{\sigma}$, $\hat{S}_+ = \hbar\hat{\sigma}^\dagger$, and $\hat{S}_- = \hbar\hat{\sigma}$, and omit the $\frac{1}{2}$ in the Hamiltonian.

[29] The two level system, or two state quantum system, might still be part of a bigger (non-degenerate) system.

Particularly interesting is the situation where the system is driven with a coherent external radio-frequent magnetic field with frequency ω_d and amplitude B_1. Because $B_1 \ll B_0$, we can neglect the direct effect on the longitudinal magnetization. For convenience let us choose $\boldsymbol{y}$ such that $B_{1_y} = 0$, and use $\Omega_1 \equiv \gamma_s B_{1_x}/2$. Hence, the Hamiltonian becomes

$$\begin{aligned}
&\hat{H} = \hat{H}_0 + \hat{H}_{1\perp} + \hat{H}_{1\parallel} + \hat{H}_{drive}, \quad \text{with} \\
&\hat{H}_0/\hbar \equiv \omega_0 \hat{a}^\dagger \hat{a} + \omega_s \hat{\sigma}^\dagger \hat{\sigma} \\
&\hat{H}_{1\perp}/\hbar \equiv \left(\hat{a}^\dagger + \hat{a}\right)\left(g_\perp^* \hat{\sigma}^\dagger + g_\perp \hat{\sigma}\right) \\
&\hat{H}_{1\parallel}/\hbar \equiv g_\parallel \left(\hat{a}^\dagger + \hat{a}\right)\hat{\sigma}^\dagger\hat{\sigma} \\
&\hat{H}_{drive}/\hbar \equiv 2\Omega_1 \cos\left(\omega_d t\right)\left(\hat{\sigma}^\dagger + \hat{\sigma}\right).
\end{aligned} \tag{5.14}$$

Going to the rotating frame to make the Hamiltonian above time-independent shows that interesting physics comes up depending on frequency ω_d. This is either due to the interaction term $\hat{H}_{1\perp}$ or $\hat{H}_{1\parallel}$, but not for the same values of ω_d. Therefore we review two situations: the first with Hamiltonian $\hat{H}_\perp \equiv \hat{H}_0 + \hat{H}_{1\perp}$ and the second with $\hat{H}_\parallel \equiv \hat{H}_0 + \hat{H}_{1\parallel} + \hat{H}_{drive}$.

THE HAMILTONIAN $H_\perp$ is particularly interesting for spontaneous interaction between the spin and resonator, thus without the external field turned on:

$$\hat{H}_\perp = \omega_0 \hat{a}^\dagger \hat{a} + (\omega_s - \omega_d)\, \hat{\sigma}^\dagger \hat{\sigma} + \left(\hat{a}^\dagger + \hat{a}\right)\left(g_\perp^* \hat{\sigma}^\dagger + g_\perp \hat{\sigma}\right). \tag{5.15}$$

Although this is one of the simplest Hamiltonians of interacting quantum systems, achieving an analytical solution for the Schrödinger equation is not easily feasible due to the fact that there is no conserved quantity other than the energy. If one takes the rotating wave approximation, the system would reduce to the Jaynes-Cumming model which has a continuous $U(1)$ symmetry. However, this approximation is only valid if $|\omega_s - \omega_0| \ll |\omega_s + \omega_0|$ and $g \ll \omega_0$. The first is definitely not a valid assumption in our system where ω_s is in the GHz regime, and ω_0 only several kHz. Moreover, it is questionable whether $g \ll \omega_0$ as we will show in the next section that g can be hundreds of Hz.

Braak[30] showed that the system can actually be solved. Although a bit different from the Jaynes-Cummings ladder state solution, level crossing of various states can still occur, enabling the transition from higher to lower phonon number states (and vice versa). It can be guessed that the typical transition rate is $g_\parallel$. Making the transition rate asymmetric by pulling the qubit into its ground state would cool (or heat) the resonator. Braak[30] showed, however, that level crossings only occur when the external transition rate is a multiple of $\omega_0/2$. This method is different from what is used in optomechanics and not fully explored in the regime where $\omega_0 \ll \omega_s$. *A thorough theoretical analysis is needed to fully explore the possibilities that the system described with this Hamiltonian might reveal.*

[30] Braak 2011

THE HAMILTONIAN $\hat{H}_\parallel$ can be made time-independent when the wave function $|\Psi\rangle \to e^{i\omega_d \hat{\sigma}^\dagger \hat{\sigma} t} |\Psi\rangle$. Then according to the

Schrödinger equation, the effective Hamiltonian is

$$\hat{H}_{\parallel} = \omega_0 \hat{a}^\dagger \hat{a} + (\omega_s - \omega_d)\,\hat{\sigma}^\dagger \hat{\sigma} + g_{\parallel}\left(\hat{a}^\dagger + \hat{a}\right)\hat{\sigma}^\dagger \hat{\sigma} + \Omega_1\left(\hat{\sigma}^\dagger + \hat{\sigma}\right), \tag{5.16}$$

where we neglected the fast oscillating terms $e^{\pm 2\omega_d t}$. This Hamiltonian is very similar to the Hamiltonian for optomechanics,[31] with the only difference that the photons from the laser (bosons) are replaced with a spin state (fermion). The main difference here is that $\hat{\sigma}^\dagger \hat{\sigma}$ is finite,[32] meaning that when the system is continuously driven, the 2LS oscillates between its states. Compared to optomechanics, we are in a special regime, the single photon regime. The otherwise nonlinear behavior[33] does not happen, because for a 2LS $\left(\hat{\sigma}^\dagger \hat{\sigma}\right)^2 = \hat{\sigma}^\dagger \hat{\sigma}$. What remains is a resonance frequency shift for the spin by $|g|^2/\omega_0$. Note that when $\omega_d = \omega_s - \omega_0$ the first two terms of $\hat{H}_{\parallel}$ are degenerate, meaning that the interaction term will let the state oscillate between a quantum state with n phonons and the spin in the ground state, and a state with $n-1$ phonons and the spin in the excited state.

[31] Aspelmeyer et al. 2014

[32] There are only two values, 0 and 1, for spin-$\frac{1}{2}$.

[33] See Aspelmeyer et al. 2014, Sec. X.F.

MANY PROPOSALS to explore the quantum regime with mechanical devices require cooling of the resonator to(wards) the ground state.[34,35,36] It is easier to do statistics on quantum measurement outcomes once the probability amplitudes are not convoluted with the thermal spectrum. Moreover, harmonic oscillators with a lower number of phonons exhibit a lower rate of decoherence.[37] As explained by Aspelmeyer,[31] the average phonon number $\bar{n}$ changes according to

$$\frac{d\bar{n}}{dt} = (\bar{n}+1)\left(A^+ + A^+_{th}\right) - \bar{n}\left(A^- + A^-_{th}\right), \tag{5.17}$$

where $A^\pm$ are the rates per phonon for upward (higher number of phonons) and downward transitions. The thermal transition rates are given by $A^+_{th} = n_{th}\frac{\omega_0}{Q}$ and $A^-_{th} = (n_{th}+1)\frac{\omega_0}{Q}$.[31] When the interaction term in the Hamiltonian is not relevant, the average number of phonons reaches an equilibrium value $\bar{n} = n_{th} \approx \frac{k_B T}{\hbar\omega_0}$ with T the temperature of the

[34] Marquardt et al. 2007

[35] Braginsky et al. 1995

[36] Marshall et al. 2003

[37] Gardiner and Zoller 2004

surrounding heat bath.

The $A^{\pm}$ transition rates can be calculated using Fermi's golden rule and following Ref. 31

$$A^{\pm} = 2\pi\hbar g_{\parallel}^2 S\left(\omega_d \pm \omega_0\right) \tag{5.18}$$

where $S\left(\omega_d \pm \omega_0\right)$ is the spectral density of the spin.[38] The transition rates are clearly different as $\omega_d = \omega_s - \omega_0$, however, the precise imbalance between the transition rates depends on the width of the distribution S.

[38] S is the spin's lineshape: a normalized distribution with units of 1/frequency and centered at ω_s, or $\omega_s - g_0^2/\omega_0$ when taking the whole Hamiltonian into account. For spin-$\frac{1}{2}$ the function is normalized. For a spin without interactions, S is a Lorentzian function with a full width at half maximum of $\frac{1}{T_2}$.

As a point of concern: *it is questionable if the results obtained from optomechanics are valid in our case. Namely, we are not necessarily in the weak coupling regime. On the other hand the polaron description as used in the strong coupling regime*[31] *might need a closer look to check if the same measurement protocols can be applied as in optomechanics.* Note that $\hat{H}_{\parallel}$ is similar to the Holzstein Hamiltonian which can be transformed into $\hat{H}_{\perp}$,[39] leaving us with the same questions as before. However, if we can manipulate the qubit in other ways, we can simply hack the transition rates by continuously pushing the qubit into a chosen state using these alternative ways, such that spontaneous transitions can only occur into the required direction. For now let us assume everything works as in optomechanics.

[39] Tayebi and Zelevinsky 2016

By setting $\frac{d\bar{n}}{dt} = 0$ and assuming $\frac{1}{T_2} \ll \omega_0$, we find the equilibrium phonon number

$$\begin{aligned} \bar{n} &= \frac{A^+ + A_{th}^+}{A^- + A_{th}^- - A^+ - A_{th}^+} \\ &= \frac{n_{th}}{C_0 + 1}, \qquad \text{with} \\ C_0 &= \frac{4g_{\parallel}^2 T_2 Q}{\omega_0}. \end{aligned} \tag{5.19}$$

If the cooperativity C_0 is larger than n_{th}, the system can be cooled to between the ground state and the first excited state. Therefore it is often more useful to work with

$$C \equiv \frac{C_0}{n_{th}} = \frac{4\hbar g_{\parallel}^2 T_2 Q}{k_B T} \tag{5.20}$$

which is an important figure of merit in optomechanical systems and other quantum hybrid systems. If we compare this boson-fermion system with a standard optomechanical setup, the cooperativity cannot be enhanced by adding more photons in the cavity as there are only two spin states. However, if the coupling is strong enough such that $C > 1$, it is easier to bring the mechanical resonator into a cat state as the quantum nature of the single qubit, in contrast to the many photons, is not averaged out.

NOW THAT THE RELEVANT INTERACTIONS are on the table, we can focus on how to construct an experiment that uses these interactions to go beyond quantum mechanics.

5.5 *The experiment blueprint*

THE PROPOSED EXPERIMENT involves the coupling between a heavy harmonic oscillator and an controllable quantum object. As argued in Ch. 1, the best suited objects with long coherence times are defects in diamonds that consists of nitrogen, an adjacent vacancy and an extra electron. These NV^--centers[40] have a particular energy level scheme that allows for precise control of the three level spin-state. The system can always be driven into the spin ground state by applying a laser pulse, see Fig. 5.4 for a graphical explanation. Depending on the follow-up research on Sec. 5.4, this feature is helpful to make the transition rates asymmetric. Furthermore, the released light is valuable as it gives information about whether the system was in the $m_s = 0$ or $m_s = \pm 1$ state.

The spin state can also be controlled by magnetic resonance. Due to the zero-field splitting that the NV-center features, see Fig. 5.5, an atypical spin-state energy splitting results as the $m_s = 0$ state has a lower energy than the $m_s \pm 1$ states. Luckily the $m_s \pm 1$ states have a different transition energy,

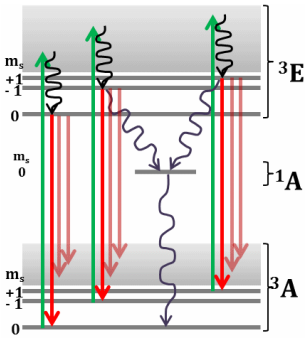

Figure 5.4: Energy level structure of an NV^--center. The $m_s = 0$ states from the ^3A and ^3E states are separated by a 637 nm-photon energy. If the states are excited with green light there is a probability that the system decays back to the same m_s value in the ^3A state (eventually via the grey sidebands), however for the $m_s = \pm 1$ states there is a significant probability that it decays to the ^1A state which is not m_s preserving. From there it falls back to $m_s = 0$. Applying the green pulse long enough will always bring the system to the $m_s = 0$ state.

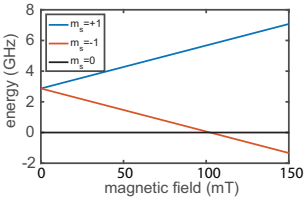

Figure 5.5: Energy of the m_s states in the optical ground state ^3A. The three level spin system has a zero field splitting of 2.87 GHz.

[40] From now on just NV-centers, or NVs.

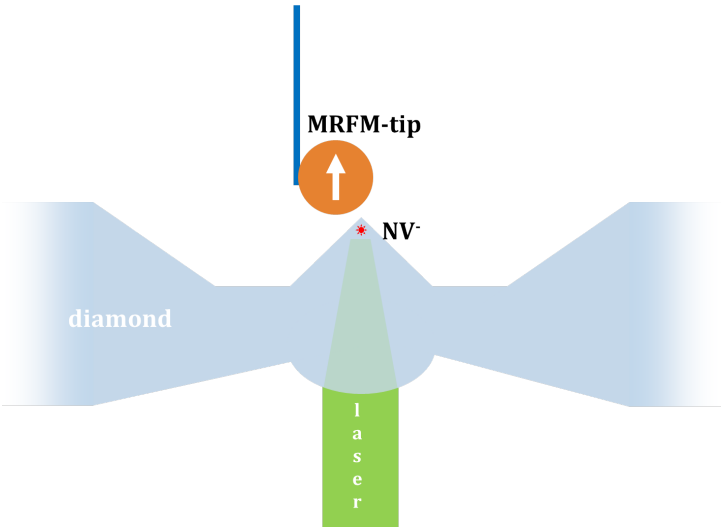

Figure 5.6: Sketch of the proposed experiment. The diamond that contains the NV-center is shaped as a cone or pyramid with 45° angles for maximal light reflection. At the same time there is plenty of space for the MRFM-tip, thereby enabling an intermediate coupling $g_\perp$ or $g_\parallel$ of order ω_0 between MRFM-tip and sample.

so we can address the transitions individually by exciting the $m_s = 0$ state with the right frequency. Because of this, and because we can always initialize the spin in the $m_s = 0$ state, we can treat the NV-center as two superimposed 2LSs.

THERE ARE two practical realizations of how we can couple the NV-center and the resonator: 1) the magnet on the resonator and the NV below, or 2) the NV on the tip and the magnet below. In both cases the magnet or NV-center cannot be positioned beside the resonating cantilever, but only below, otherwise the soft cantilever would snap to contact.
The first realization, the magnet-on-tip method, is the one used in Chs. 3 and 4. The advantage is that the magnet is not only useful for the coupling between resonator and spin, but its motion can also be detected by SQUID-readout.[41] Remember that measuring the motion of the resonator with a laser is not an option as inevitable absorption of the light will raise the temperature of the resonator. For controlling the NV, however, we do need laser light in the experiment. The pulses are typically 1 μs or less with $0.1 - 10$ mW laser power. If we apply one pulse per cantilever oscillation, the induced

power into the experiment is in the order of μW. The laser power can be reduced by using on-resonance laser pulses (637 nm), which reduces the needed power by three orders of magnitude.[42] The drawback of this method is the possible bleaching of the NV^--center to the useless NV^0-center.[43] The laser power that hits the resonator can also be lowered by using a reflector between the spin and the magnet. A mirror is, however, not an option as a dielectric mirror would be too thick and a metal one will give rise to eddy currents. Luckily due to the high refractive index of diamond[44] we can construct a corner reflector as shown in Fig. 5.6. There is no need to use reflective coatings or other mirrors providing that the incoming beam is parallel enough. The critical angle for total internal reflection for the diamond-vacuum interface is 24.4°. The incoming angle of the beam shouldn't divert more than 20.6° from the ideal 45° to both interfaces. An advantage of having a parallel beam is that the laser beam's mode is not distorted, which leads to a higher collection efficiency of photons into the fiber and thus less heating.

There are more reasons why a pyramid-shaped diamond feature would be better than a simple flat surface: the coupling between the NV-center and the resonator is very small when the magnet is right above the NV-center, but it is maximal when it is positioned a bit off-center as shown in Fig. 5.6. Due to the pyramid shape the magnet can come closer to the NV-center without touching the surface. A risk of this particular shape is that the cantilever might be pulled towards the pyramid because of electrostatic or Van der Waals forces.
On the other hand, however, due to the reduced amount of diamond bulk and surface in the neighborhood of the MRFM-tip, it interacts less with the unwanted two level fluctuators on the surface which leads to less dissipation, see Chs. 2-4.
For a NdFeB magnet of 3 μm diameter, such as typically

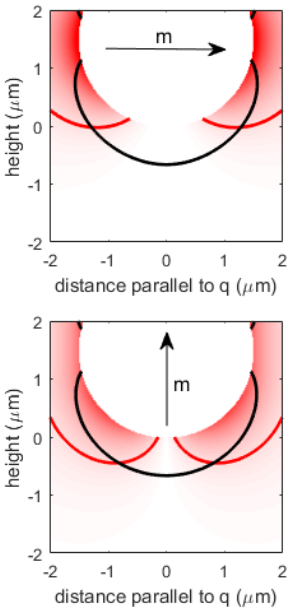

Figure 5.7: Shown are the magnetic field gradients that are relevant for the interaction strength. The magnet is magnetized in q-direction (top figure) and in height direction (bottom figure). In red the gradient component in direction of the magnetic field is shown, and in black the component perpendicular to the magnetic field. Both contour lines are given for 0.2 T/μm. The perpendicular component does not depend on the direction of magnetization (but it does depend on the direction of q). The position of the qubit would ideally be chosen inside the area enclosed by the black and red line, and the magnet. Therefore a magnetization in the height direction seems to be more suitable.

[41] Usenko et al. 2011
[42] Robledo et al. 2010
[43] Manson and Harrison 2005
[44] The refractive index of diamond is 2.42.

used in Chs. 2-4, we can easily achieve magnetic field gradients of 0.2 T/μm if the qubit is well positioned as shown in Fig. 5.7. With the ultrasoft silicon cantilevers that have a spring constant of 50 μN/m and an electron spin, the interaction strength g_0 is about 0.8 kHz. Together with a Q of 10^4 and an T_2 of 1 ms, we find a single phonon cooperativity $C \approx 250$.

Due to the softness of the cantilever, the zero point motion is 141 fm which is relatively large compared to other optomechanical experiments.[31] However, note that the temperature corresponding to the ground state energy is extremely low with a value of only 72 nK.

THE OTHER REALIZATION with the NV on the tip of the resonator has several advantages and challenges. One of the main problems is the readout of the resonator. Since the detection of the motion cannot be done optically due to excessive heating, then practically it should be done with either the static electrical field or magnetic field.[45] It is advantageous to not have a magnet on the tip of the resonator to make the hybrid quantum system insensitive to stray magnetic fields that are difficult to avoid. It is much easier to shield the system from an electrical field. Detecting the static electrical field, like a SQUID did for the magnetic field, can be done with single electron transistors or similar devices exploiting the Coulomb blockade.[46] A problem with this method is the relatively high dissipation of these devices compared to SQUIDs.

[45] Static here means varying slower such that the wavelength is much longer than the typical size of the system.

[46] Okazaki et al. 2013

Another problem would be the need of a laser interacting with the NV-center. The coupling could be done by putting the diamond containing NV particle close to an optical waveguide and let it interact with the evanescent field.[47] Although it still seems subject to heating, keep in mind that also in the magnet-on-tip situation the magnet is so close to the pyramid that it also can couple to the evanescent field.[48] *The question*

[47] Fu et al. 2008

[48] Patel et al. 2016

is whether the heating due to optical modes on the magnet's surface in the magnet-on-tip situation isn't worse for heating than the optical electrical field heating up the diamond in the diamond-on-tip situation.

Beside the insensitivity of this method to stray magnetic fields, a big advantage of this realization is that the magnetic field does not have to be generated by a magnetic particle, but can be controlled using thin crossed electrical lines for generating the magnetic field in the wanted strength and direction.[49]

[49] Nichol et al. 2012

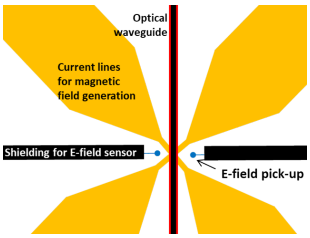

Figure 5.8: Sketch of structures that are needed on the detection chip for a NV-on-tip realization. The optical waveguide for wavelengths of ∼637 nm are needed to control and probe the NV-center. The generators for the magnetic field can magnetize the NV-center by a DC-current that is flowing through them, and flip the spin if the current is radio frequent. The voltage of the shielded lines would change if the cantilever-tip has a high voltage with respect to the shielding, and the tip oscillates. The position readout is then performed by sensing the electric field that these lines generate using single electron tunneling devices that consist of quantum dots that are tuned very sensitively to the electrical field.

5.6 Roadmap and outlook

THE PROPOSED REALIZATIONS are promising candidates for experiments that might explore the macroscopic boundaries to quantum mechanics when it comes to large mass, large displacement. The protocols to bring the system in a cat state depend on the precise realization. Moreover, the detection methods applied will decide the best way to do the quantum statistics and check whether the system is in the quantum regime, or whether it is collapsed/decohered to a classical state. The collapse/decoherence time as function of the superposition separation, the mass of the cantilever tip, and the distance to earth are the holy grails of these experiments. It is, however, not straightforward to measure such a curve and indirect measurement methods might be needed to obtain the same information. For example, the measurement of spontaneous heating as explained in Sec. 5.3 would provide a simple, although not unambiguous, measurement of the collapse time.

NEVERTHELESS, the first steps on the route to these measurements are straightforward. The exploration and optimization of the control and detection methods while and after building the experiment of Fig. 5.6 or Fig. 5.8 would be the first priority. Before the NVs and the resonator are combined in

one setup, one can already optimize the detection method of the tip displacement[50] and the control of the NV-center. After combining the NV-center part with the mechanical resonator part, the NV can be used as magnetometer to measure the magnetic field profile which can be used to position the NV close to the magnet. Measurements of this type are already done by Kolkowitz et al. 2012. Moreover they could detect the resonator's displacement and thermal spectrum exploiting NV-centers. This demands superb control of the NV-centers without disturbing the resonator. The upside is that this experiment can be started at room temperature which means a much faster iteration process to optimize the experiment.

[50] The SQUID readout for displacement detection is optimized during the work done for this thesis. See also Ch. 6.

Naturally, the next step would be to measure a single NV-center doing MRFM improving on the measurements of Ch. 4. Measuring a single electron spin can be done in the footsteps of the methods from Rugar et al. 2004. However, nowadays more advanced protocols are available which accelerates the measurements.[51,52] Moreover, using the feature that the NV-center can be very precisely controlled, the extensive averaging of measurement data that was necessary in 2004 will be minimal or can even be avoided.

[51] Poggio and Degen 2010

[52] Cardellino et al. 2014

If everything works, we approach rapidly the most interesting regime. At this point it is straightforward to test the methods of active feedback cooling.[53] More challenging are the different ways to do sideband cooling, as explained in Sec. 5.4, especially if spontaneous heating spoils the pure quantum interactions. At this point detailed simulations of expected signals are needed to recognize the signatures of the various mechanisms that come into play. Even more so if one tries to generate cat states. However, whatever comes out of these experiments may be interesting for various branches in physics. We can conclude that we are on the doorstep of exciting times; technologically for creating macroscopic

[53] Vinante et al. 2012

quantum systems, theoretically for testing the boundaries of quantum mechanics and finding experimental directions for unifications of fundamental theories, and, hopefully, an unequivocal interpretation of quantum mechanics that amends our worldview in a consistent matter.